Carbon 163 (2020) 95–104

Contents lists available at ScienceDirect

Carbon

journal homepage: www.elsevier.com/locate/carbon

Fundamental limitations in transferred CVD graphene caused by Cu catalyst surface morphology

Benjamin Huet [a, b, c, *], Jean-Pierre Raskin [d], David W. Snyder [c], Joan M. Redwing [a, b]

[a] 2D Crystal Consortium (2DCC), Materials Research Institute (MRI), The Pennsylvania State University, University Park, PA, 16802, United States
[b] Department of Materials Science and Engineering, The Pennsylvania State University, University Park, PA, 16802, United States
[c] Applied Research Laboratory (ARL), The Pennsylvania State University, University Park, PA, 16802, United States
[d] Electrical Engineering department (ELEN), Université catholique de Louvain (UCL), Louvain-la-Neuve, 1348, Belgium

ARTICLE INFO

Article history:
Received 28 January 2020
Received in revised form
24 February 2020
Accepted 25 February 2020
Available online 6 March 2020

Keywords:
Chemical vapor deposition
Cu catalyst morphology
Epitaxial Cu film
Wet transfer
Strain
Doping
Cracks
Wrinkles
Ripples

ABSTRACT

The transfer of large-area graphene is a critical step in the development of technological applications, particularly when its structural integrity and physical properties are of central importance. While the scientific community dedicated a great deal of efforts improving the scalability and cleanliness of the transfer protocol, less research focused on the fundamental mechanisms responsible for the formation of cracks, wrinkles, corrugations, folds and mechanical strain which drastically hinder the reliability of the process. Here we describe how the surface morphology of copper, which serves as catalyst for the graphene chemical vapor deposition (CVD), significantly impacts (i) the transfer process reliability, (ii) graphene's planar aspect, and (iii) graphene's physical properties once transferred onto device-compatible substrates. We systematically compare the transfer of highly crystalline graphene from Cu foils, polycrystalline Cu films and epitaxial Cu films which possess a surface roughness spanning over 2 orders of magnitude. Our results suggest that, regardless of the transfer approach, the Cu template surface morphology is one of the major causes for the non optimal transfer results and discrepancies in physical properties reported in the literature. These findings provide valuable insights encouraging the use of alternative substrates when considering the integration of graphene into functional applications.

1. Introduction

Graphene has been the subject of fervent global research over the last 15 years because of its two-dimensional (2D) nature and its exceptional physical properties [1–3]. Although it has been regarded as a versatile material capable of reshaping tomorrow's technology, graphene has yet to deliver on its promises. While the scientific community continues to be optimistic, it also realizes the complexity of fully harnessing graphene's great potential once integrated into functional applications [4–6]. Synthesizing pristine graphene, which is at the essence of device development and cutting-edge fundamental research, does not seem to be the main hurdle anymore given the latest chemical vapor deposition (CVD) progress [7,8]. The CVD of graphene on Cu substrates is certainly one of the most advanced and industrially viable manufacturing techniques as it is cost-effective, scalable and offers a good control over the number of layers and structural quality [9]. The great success of the CVD of graphene on metal catalysts has been followed by a staggering surge of research activity aiming at developing an effective, scalable, and reliable transfer technique which meets the requirements for device fabrication and industrialization [10].

The library of transfer methods has been greatly expanding since Kim et al. demonstrated the first transfer of CVD-grown graphene in 2008 [11]. Most transfer protocols reported in the literature involve the following steps: (i) deposition of a temporary mechanical support on top of graphene, (ii) separation of graphene from the synthesis substrate, (iii) deposition of graphene/support on the final substrate and, (iv) mechanical support removal. These protocols mainly differ by the nature of the mechanical support (e.g. polymethyl methacrylate (PMMA) [12,13], Polydimethylsiloxane (PDMS) [11,14], polystyrene (PS) [15], cyclohexane [16], ethylene vinyl acetate (EVA) [17], or paraffin [18]), the separation technique of graphene from the catalyst (e.g. wet

* Corresponding author. 2D Crystal Consortium (2DCC), Materials Research Institute (MRI), The Pennsylvania State University, University Park, PA, 16802, United States.
E-mail address: benjamin.huetb@gmail.com (B. Huet).

https://doi.org/10.1016/j.carbon.2020.02.074
0008-6223/

etching [12,19] or bubbling [20]), the graphene deposition approach (e.g. wet fishing [12] or dry elastomer stamping [21–23]), and the support layer removal (e.g. dissolution in solvent [12] or mechanical peeling [23]).

These various derivatives have been devised with the aim of reliably transferring large areas of graphene with minimal physical degradation, limited contamination by polymeric residues from the supporting layers or metallic particles from the catalyst etching process, and no graphene functionalization induced by aggressive chemicals. Unfortunately, none of the aforementioned methods concomitantly addresses all these issues yet and meets the strict requirements for the large-scale integration and industrialization. Another problem, which has been overlooked so far, is the role of the Cu substrate in the reliability, repeatability and quality of the transfer. The planar aspect of CVD-grown graphene strongly depends on the catalytic Cu template as the growth mimics the underlying surface morphology [24]. The supporting layer mechanically reinforces the atomically thin layer and helps maintaining graphene's structural integrity once released from the synthesis substrate. Unfortunately, it also forms a hard cast that maintains graphene planar aspect during the transfer process. The Cu substrate morphology imprint in the supporting layer prevents a uniform contact of graphene on the final substrate, drastically impairs the van der Waals forces, and ultimately makes graphene more prone to detach and be washed away during the support removal step [25].

In this work, we systematically compare the transfer of CVD graphene grown on different catalytic substrates including Cu foils, polycrystalline Cu films, and epitaxial Cu films. This study is based on the wet PMMA-assisted transfer method which is easily scalable and widely employed among the scientific community. It is shown that the Cu surface morphology, which strongly differs from one type of Cu substrate to another, impacts the transfer reliability and quality. It is shown that decreasing the Cu surface roughness results in a more conformal deposition of graphene on the final substrate, a better adhesion and hence, less graphene degradation (tears, holes, folds, …) upon the PMMA removal step. We also demonstrate that more planar Cu substrates also lead to a lower density of wrinkles and limits the formation of localized mechanical strain and doping in transferred graphene. Finally, we show that the Cu surface crystallographic orientation plays a key role in graphene's planar aspect and its ability to interact with the underlying final substrate once transferred. Our results suggest that a flat and smooth epitaxial Cu film represents the most promising template to obtain uniform continuous high-quality graphene once transferred on arbitrary surfaces.

2. Results & discussions

2.1. Cu surface morphology

Over the last decade, graphene has been successfully produced on various types of catalytic substrate including Cu foils, polycrystalline Cu films, epitaxial Cu films and even Cu plates [26]. Although Cu foils have been the predominant choice for the scientific community, a few research groups demonstrated the growth of graphene on Cu films pre-deposited on fused quartz [7,9,27], oxidized Si [28,29], mica [30], MgO [31] and sapphire [9,32–35] wafers. Upon the CVD process, the high temperature induces the re-crystallization of the Cu substrate and drastically modifies its surface morphology. Cu foils and Cu films pre-deposited on amorphous substrates (e.g. fused quartz, SiO_2/Si) lead to the formation of a grained microstructure [7,32]. In contrast, thin Cu films pre-deposited on crystalline wafers exhibiting a small lattice mismatch (e.g. mica, MgO, α-Al_2O_3) result in a single-crystalline Cu film [9,32,34].

For this study, highly crystalline graphene (Gr) is grown on Cu foils, polycrystalline Cu film and epitaxial Cu films using CVD conditions similar to those reported in previous reports [7,8,32]. Non-coalesced millimeter-size single-crystalline graphene domains are grown in order to avoid the formation of graphene grain boundary-induced defect lines and more easily realize if defects are caused during the growth or during the transfer processes. Large compact domains also serve as visual guide to correlate the Cu substrate surface features with graphene features once transferred on the final substrate. After the CVD process, the as-grown Gr/Cu substrates are heated up for a few tens of seconds on a hot plate at 200 °C in air to make graphene visible [36].

Fig. 1 shows optical microscope images, 3D optical profilometer images and 2D profilometer scan lines of the surface of a 50 μm-thick Cu foil, a 2.4μm-thick Cu film on fused quartz and a 1.0μm-thick Cu film on C-plane sapphire after graphene growth. Cu substrate surface features such as grain boundary grooves or cold-rolling striations (in the case of Cu foils) contribute to the Cu template waviness and roughness, and hence adversely impact graphene planarity. The Cu surface morphology has been assessed by acquiring eight 167 $\times$ 167μm^2 3D optical profiles in random locations on each type of Cu catalyst (Zygo NexView, x50 lens). Cu foil surface exhibits an arithmetic average roughness S_a and a root mean square roughness S_q in the 360–990 nm and 440–1190 nm ranges, respectively. This roughness represents about one order of magnitude higher than polycrystalline Cu films (S_a:90–150 nm, S_q:157–197 nm) and about two order of magnitude higher than epitaxial Cu films (S_a:9–11 nm, S_q:11–13 nm). The significant difference in surface roughness mainly arises from the presence of Cu grain boundary grooves which are non-existent on epitaxial Cu films but can reach a depth of about 2200 nm for polycrystalline films and about 7 μm for Cu foils. Additional 3D surface profiles can be found in Supporting Information S1.

2.2. Transfer reliability

After the graphene growth process, the Cu substrates are spin-coated with PMMA (MicroChem, 950A, 3% in anisole, 2000 rpm, 60 s) to obtain a mechanical support with a thickness of about 150 nm. The PMMA is dried at room temperature in air for at least 3 h before the Cu etching step. Cu etching is achieved using $FeCl_3$ diluted in deionized (DI) water (1:1). Once the Cu is completely etched away, the $FeCl_3$ solution is gradually replaced by DI water. The Gr/PMMA sheet is transferred in 4 successive DI water baths in order to achieve sufficient rinsing and then scooped with a 90-nm thick SiO_2/Si substrate (Addison Engineering Inc., USA). The sample is air dried at room temperature for at least 24 h to ensure that most of the water at the Gr/SiO_2 interface is removed. Fresh PMMA is redeposited in order to soften the PMMA hard cast, improve the contact between graphene and the underlying substrate, and make it less prone to degradation upon the PMMA removal step [25]. The liquid PMMA solution is kept on the sample for about 40 min before immersing the sample in an acetone bath which is then heated up to and maintained at 50 °C for 2 h. The Gr/SiO_2/Si sample is then rinsed with clean acetone and isopropanol before being dried with a nitrogen spray gun. Supporting Information S2 shows transferred graphene results when failing to properly rinse graphene, using a thicker PMMA film, or not softening the PMMA cast prior to its removal.

Upon the spin-coating of the mechanical support on top of graphene, PMMA fills in the deep Cu grain boundary grooves and form a hard cast with the imprint of the Cu surface morphology. Once the Gr/PMMA stack is isolated from the Cu substrate, carefully rinsed and scooped by the final substrate, a thin film of water gets

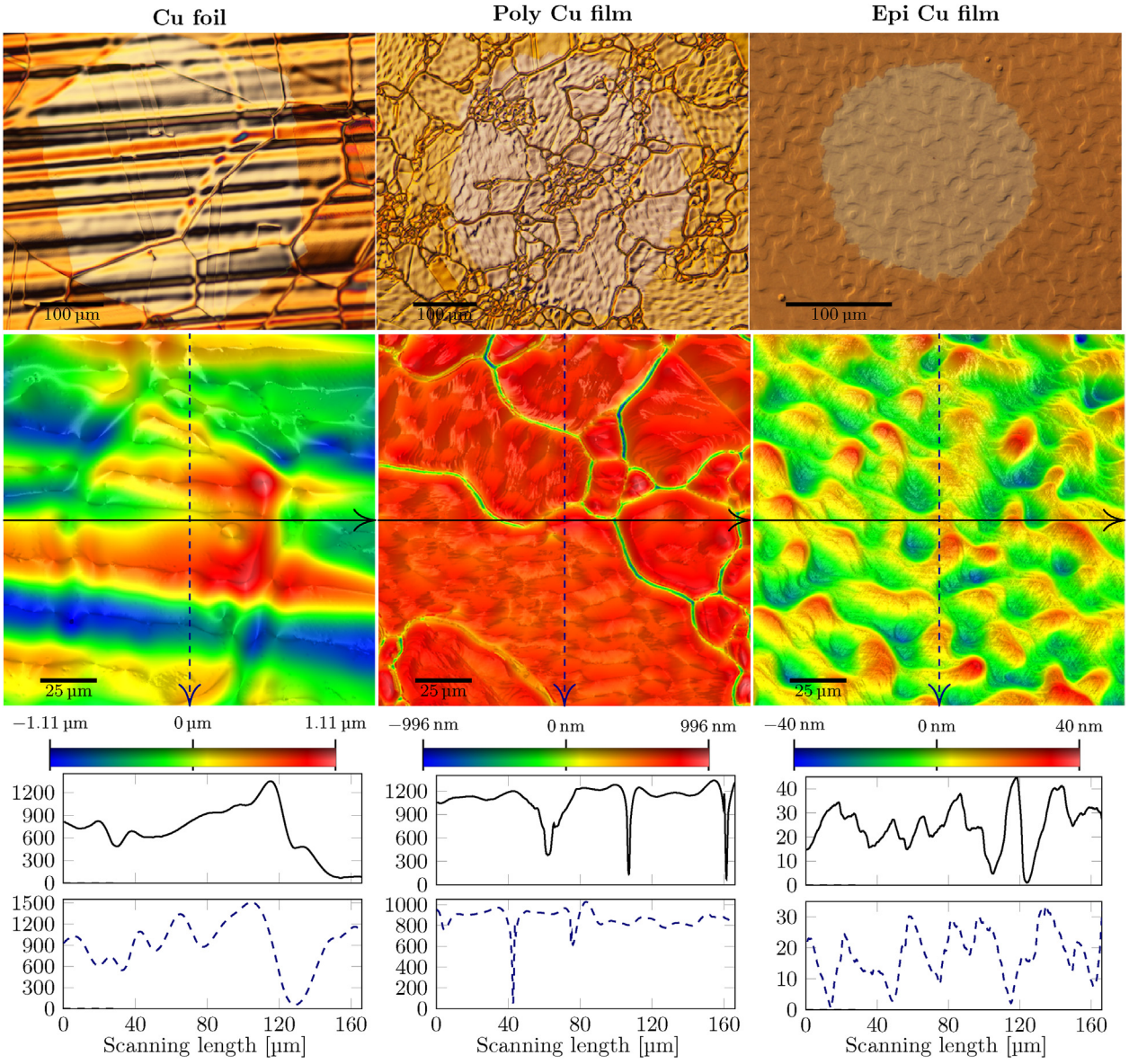

Fig. 1. Comparison of the Cu surface morphology of Cu foil (**left column**), polycrystalline Cu film (**middle column**) and epitaxial Cu film (**right column**) after graphene growth. **Top panel:** Optical microscope images of a single crystal of graphene after a slight oxidation to make it visible. Differential Interference Contrast (DIC) is used to enhance surface morphology effects. **Central panel:** 3D optical profilometer images. **Bottom panel:** 2D sections along the arrows displayed in the 3D profiles in the central panel. Solid black (top) and dashed blue (bottom) profiles correspond the horizontal and vertical arrows, respectively. (A colour version of this figure can be viewed online.)

trapped at the Gr/substrate interface. This water plays a critical role in the transfer as the capillarity forces pull the Gr/PMMA stack down in close contact with the underlying substrate. This close contact is a key factor determining the reliability of the transfer as graphene adhesion only arises from van der Waals forces [37]. When graphene does not come into close contact with the underlying substrate, solvents employed to remove the supporting PMMA layer penetrate underneath graphene and tear it away. The ability of graphene to come into close contact with the substrate mostly depends on the PMMA bending stiffness (i.e. the layer thickness) and the Gr/PMMA surface morphology. Thin PMMA film thickness can be easily decreased by further diluting PMMA in anisole or by increasing the rotation speed of the spin coater. Very thin films ($\lesssim$80 nm) are however more difficult to handle and are likely to contain voids when deposited on substrates with high surface roughness. The Gr/PMMA surface morphology is however pre-determined by the Cu template and cannot really be improved during the transfer process.

Fig. 2 compares the transfer of graphene grown on polycrystalline Cu foil (top panel) and on polycrystalline Cu film (bottom panel). The left column shows the Gr/PMMA stack after being deposited onto a 90 nm-thick SiO_2/Si wafer and left to dry overnight in air at room temperature. The wide spectrum of colors in the optical images either indicates a non-uniform PMMA layer thickness or a varying spacing at the graphene/SiO_2 interface. Spacings, which are recognizable through the presence of closed-packed interference patterns, are typically present near the imprints of deep Cu grain boundary grooves.

By comparing the top and bottom panels, it can be observed that grain boundary grooves of Cu films lead to larger spacings than those of Cu foils. The size of these spacing is mainly dictated by the width-to-depth aspect ratio of Cu grain boundary grooves which

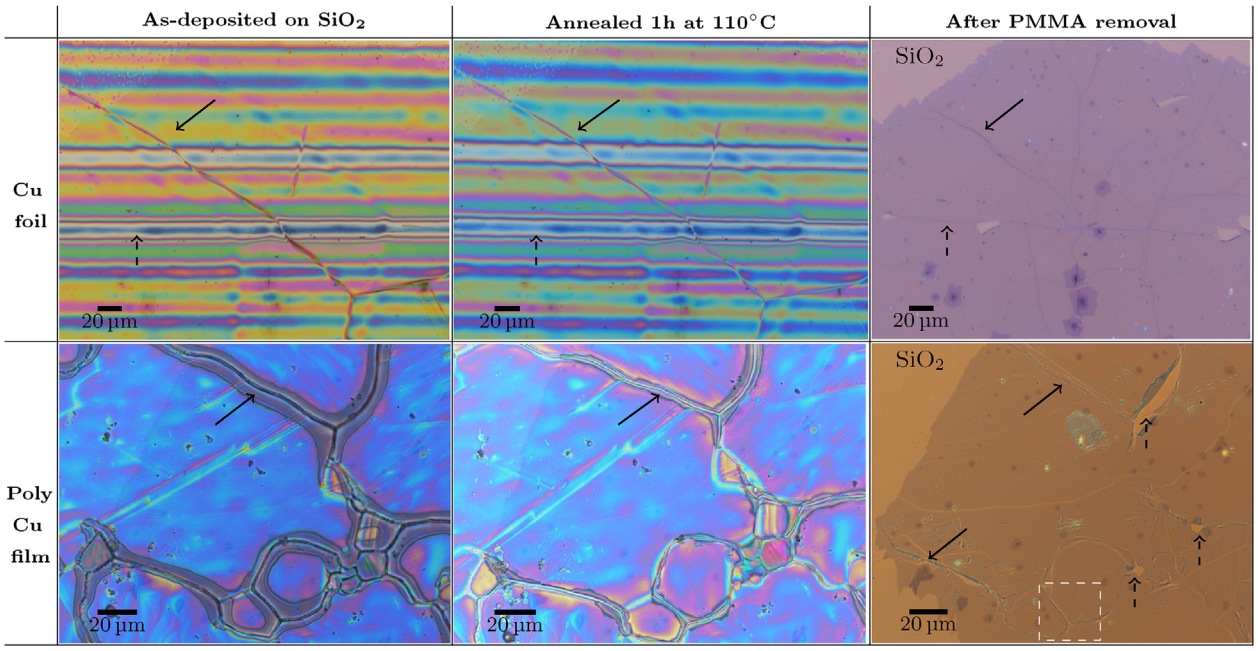

Fig. 2. Comparison of the transfer graphene grown on Cu foils (**top panel**) and on thin Cu films (**bottom panel**). **Left column**: PMMA/Gr on SiO_2/Si after drying for 24 h at room temperature. **Center column**: PMMA/Gr on SiO_2/Si after annealing PMMA/Gr at 110 °C for 1 h. **Right column**: graphene on SiO_2/Si after re-depositing fresh PMMA and removing PMMA in acetone. (A colour version of this figure can be viewed online.)

form rigid PMMA protrusions (see the bottom panel of Fig. 1). The spacings can be mitigated by heating the PMMA film above its glass transition temperature (104 °C) as shown in the center column of Fig. 2 [12]. Maintaining the PMMA/Gr/SiO_2 sample at 110 °C for 1 h softens the PMMA film and promotes the graphene/SiO_2 contact but it is not effective enough to fully eliminate the spacings in the vicinity of the high aspect ratio Cu groove imprints. Although it is a commonly used process step, heating the sample with the Gr/PMMA on its top tends to make PMMA more resistant to acetone during the PMMA removal step. Moreover, it also increases the volume of the air (or turn trapped water into vapor) in the gaps which then percolates at the interface to agglomerate into larger gas pockets which tends to damage graphene (see Supporting Information S2). Such phenomenon is more critical with increasing sample size as it becomes more difficult for trapped vapor to leave the interface. A more gentle and efficient method consists of re-depositing fresh PMMA in order to more effectively soften the PMMA and push the graphene down in contact with the underlying substrate [25]. The right column in Fig. 2 shows the result after re-depositing fresh PMMA (3% in anisole), letting it sit for 40 min, and immediately removing the PMMA in acetone.

Owing to the good optical contrast provided by the 90-nm thick SiO_2/Si substrate, graphene features can be clearly observed. Although as-grown CVD graphene already contains cracks and wrinkles [32], the transfer process introduces additional wrinkles, cracks, tears, and folds in graphene. In the case of Cu foils, only the deepest Cu grain boundary grooves and cold-rolling striations lead to the formation of wrinkles as shown by the top panel in Fig. 2 (right column). The dashed vertical arrows in the top panel of Fig. 2 show the only optically visible wrinkle induced by the striation in this area, which suggests that the striation-induced periodic waviness does not systematically create spacings, adversely influence the contact of graphene on the SiO_2 surface, and ultimately cause the formation of any optically visible wrinkles. Only the deeper Cu foil grain boundary grooves lead to visible wrinkles as shown by the solid black arrow. In the case of polycrystalline Cu films, the high aspect ratio of the Cu grooves consistently leads to tall wrinkles that have a blueish color (as indicated by black solid arrows). Tall wrinkles are typically at the origin of cracks, folds, and tears as they have a lower adhesion to the substrate underneath and can be washed away during the PMMA removal step. This can be observed in the bottom panel and right column of Fig. 2 (see dashed arrows).

Graphene grown on epitaxial Cu films seems to yield the best results in terms of transfer reproducibility and reliability. The superior flatness and complete absence of Cu grooves lead to an improved and uniform contact between graphene and the SiO_2/Si substrate surface, even without any additional PMMA softening step. Fig. 3 shows the Gr/PMMA film directly after deposition on the SiO_2/Si substrate and after the PMMA removal. The relatively long wrinkles present in the PMMA/Gr film (as shown by black arrows in the top panel of Fig. 3) are in this case not the result of the Cu surface morphology but rather caused by a poor spreading of Gr/PMMA sheet over SiO_2 surface during the scooping step, which is typical in wet transfer processes on surfaces that are not highly hydrophilic.

2.3. Strain and doping gradients

The strain present in transferred graphene can have various origins. First, as-grown graphene exhibits a non-uniform biaxial physisorption strain caused by its lattice mismatch with the underlying Cu catalyst [38]. Additional biaxial strain also develops in graphene when the CVD furnace cools down to room temperature since graphene synthesis takes place at high temperature (~1050 °C) and there is a non-negligible difference of thermal expansion coefficient between graphene and its synthesis substrate [32]. The spontaneous formation of wrinkles helps mitigate this strain but non-homogeneous adhesion of graphene on the underlying substrate only leads to a limited and localized strain relaxation [32,39]. Although it is often assumed that the remaining strain gets mostly relaxed once the graphene/polymer stack is detached

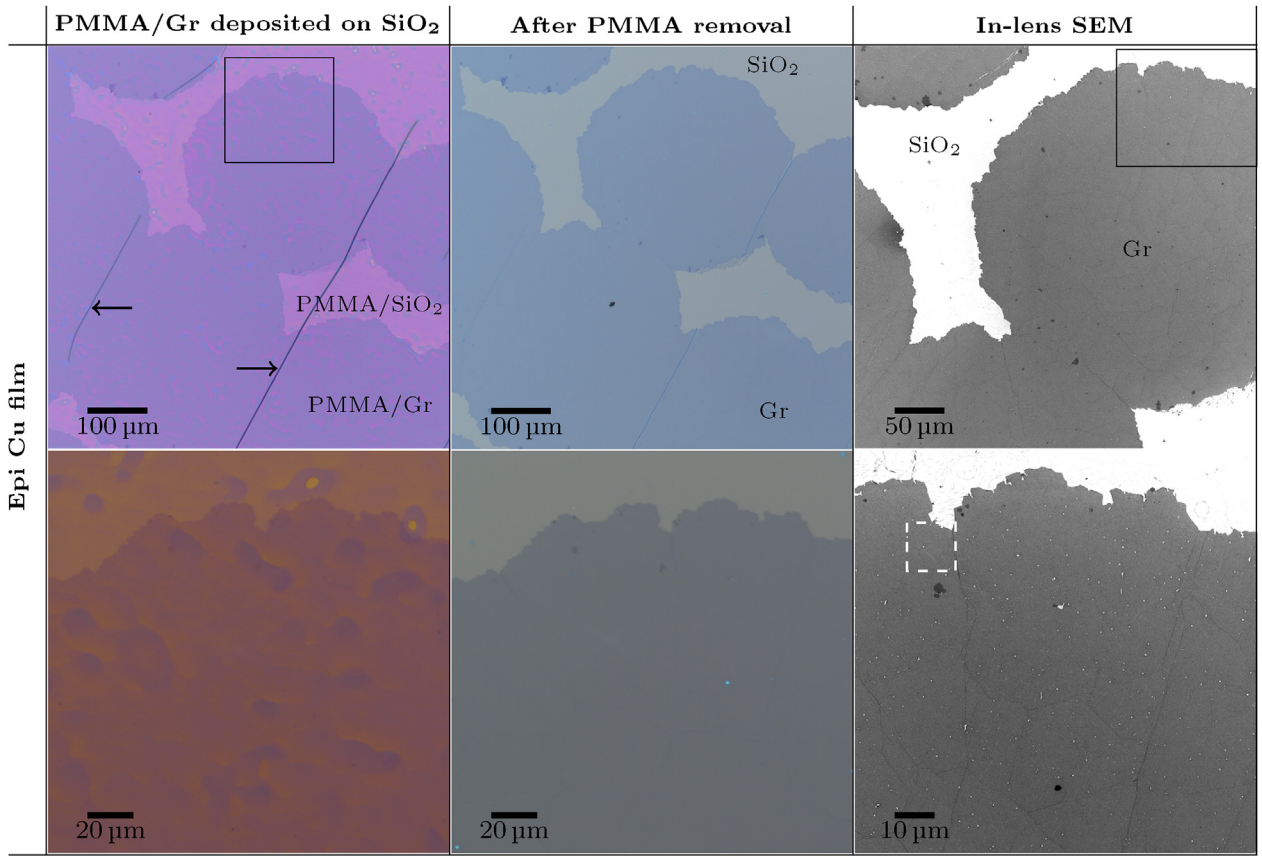

Fig. 3. Left column: PMMA/Gr deposited on SiO_2/Si after drying at room temperature for 24 h. **Center column**: graphene on SiO_2/Si after re-depositing fresh PMMA and removing the PMMA in acetone. **Right column**: in-lens SEM image of Gr deposited on SiO_2/Si after PMMA removal. **Bottom panel**: higher magnification images of the areas indicated by black squares in top panel images. (A colour version of this figure can be viewed online.)

from the Cu substrate [40], the presence of the relatively thick PMMA cast drastically limits the stress relaxation [17]. Moreover, mechanical supports made of spin-coated or drop-casted polymers most likely cause additional stress which develops during the polymer drying or curing process [41]. Determining the magnitude and direction of the strain in graphene right before its transfer on the target substrate is beyond the scope of this study as it depends on a multitude of process parameters. This study however discusses the role of the Cu surface morphology in the formation of supplementary strain in transferred graphene.

The developed interfacial area ratio (S_{dr}), which is defined as the increase in surface area caused by the roughness, constitutes an important Cu substrate metric to consider when transferring graphene. It represents the difference between the true/actual/measured Cu surface area and the projected surface area. S_{dr}, which is expressed as a percentage of additional surface, is calculated according to

$$S_{dr} = \frac{S_{Cu} - S_{projected}}{S_{projected}}. \quad (1)$$

Such Cu substrate metric corresponds to the additional surface area of graphene compared with the surface area of the target substrate covered by the PMMA cast:

$$S_{dr} \sim \frac{S_{graphene} - S_{target}}{S_{target}}. \quad (2)$$

Consequently, S_{dr} determines the ability of graphene to accommodate the final substrate surface morphology which typically possesses a surface roughness inferior to 2 nm.

The lack of planarity in graphene thus results in the development of a non-uniform biaxial mechanical strain and wrinkles of various heights and densities depending on the relaxation mechanisms in play. Based on eight $167 \times 167 \mu m^2$ 3D optical profilometer measurements acquired at random locations of each type of Cu substrate, the developed interfacial area ratio is found to be around 0.67±0.52%, 1.8±0.5% and $1.04 \pm 0.21 \times 10^{-3}$% for Cu foils, polycrystalline Cu films and epitaxial Cu films, respectively. These data suggest that graphene grown on polycrystalline Cu films possesses a greater excess of surface area than graphene grown on Cu foils, despite the surface waviness induced by the cold-rolling striations and the few micrometers-deep Cu grain boundary grooves. This result can be explained by the fact that polycrystalline Cu films have smaller Cu grains (lateral dimensions ranging from 5 to 300μm) and thus a higher density of Cu grain boundary grooves than Cu foils. This additional surface area can be easily noticed by examining the sections of the 3D scans at the bottom panel of Fig. 1.

To demonstrate that the type of Cu substrate and/or the Cu surface morphology play a role in the presence of mechanical strain in transferred graphene, we compared the Raman spectroscopy data acquired on graphene transferred from Cu foils and epitaxial Cu films. Raman spectroscopy is considered as a versatile tool to characterize graphene as it can assess the number of layers, the density of defects, the doping level, and even the in-plane strain [43]. Raman signatures of graphene typically present three dominant features: the D, G, and 2D bands which are located at about 1350 cm^{-1}, 1590 cm^{-1}, and 2680 cm^{-1}, respectively. A particular attention is given to the G and 2D bands for which the peak

positions (ω_G and ω_{2D}) and full-width at half-maximum (FWHM) (Γ_G and Γ_{2D}) are sensitive to variations of charge doping and C–C bond lengths. Spatially resolved Raman measurements have been acquired using a confocal LabRam HR Evolution (Horiba) with a 532 nm excitation wavelength, a x100 magnification lens (Na = 0.9, WD = 0.2 mm), and a power density of about 2 mW. A 1800 grooves/mm grating is employed to precisely measure the width and positions of the Raman features.

The spatial variation of strain is first investigated using graphene grown on Cu foil and transferred on 90 nm-thick SiO_2/Si. Fig. 4 shows side-by-side images of graphene before and after the PMMA removal step. The scanning electron microscope (SEM) provides valuable insights into the planar aspect of graphene as it shows cracks, wrinkles but also remnants of Cu grain boundary grooves and nanometer-scale step edges. These observations prove that even smaller Cu surface features imprinted into the PMMA/Gr stack do not flatten once the PMMA is removed and graphene is self-standing on the final substrate.

Raman mapping (19x17 = 323 data points) was conducted over the entire SEM field of view shown in Fig. 4c which covers a surface area of $54 \times 48\ \mu m^2$. Fig. 4d and e show the maps of 2D-to-G peak intensity ratio and 2D bandwidth Γ_{2D}, respectively. The 2D-to-G peak intensity ratios ranging from 1.4 to 4.3 and the highly symmetrical 2D bands (data not shown) are good indicators confirming the single layer nature of graphene which can also be observed in Fig. 4b–c. The broadening of the 2D band is usually indicative of a strain gradient within the Raman laser spot which provides a spectral average over $\sim 1\mu m^2$ [44]. Although the Γ_{2D} values measured here are similar to what has been reported in the literature for graphene on SiO_2/Si [45], they span over a fairly large range ($\sim 10\ cm^{-1}$). Interestingly, the lowest values of Γ_{2D}, for most part, coincide with the location of the Cu grain boundary grooves. This suggests that graphene is most likely locally lifted from the substrate, does not experience the effect of the SiO_2 surface roughness, and is more prone to re-distribute short-range stress gradients.

Additional maps have been acquired on graphene samples transferred on SiO_2/Si from both epitaxial Cu films and polycrystalline Cu foils. By comparing maps from different samples, it is found that graphene from epitaxial Cu film consistently exhibits 2D bands with higher Γ_{2D} values but spanning over a narrower range (see Fig. 4f and g). The more consistent but higher nanoscale strain

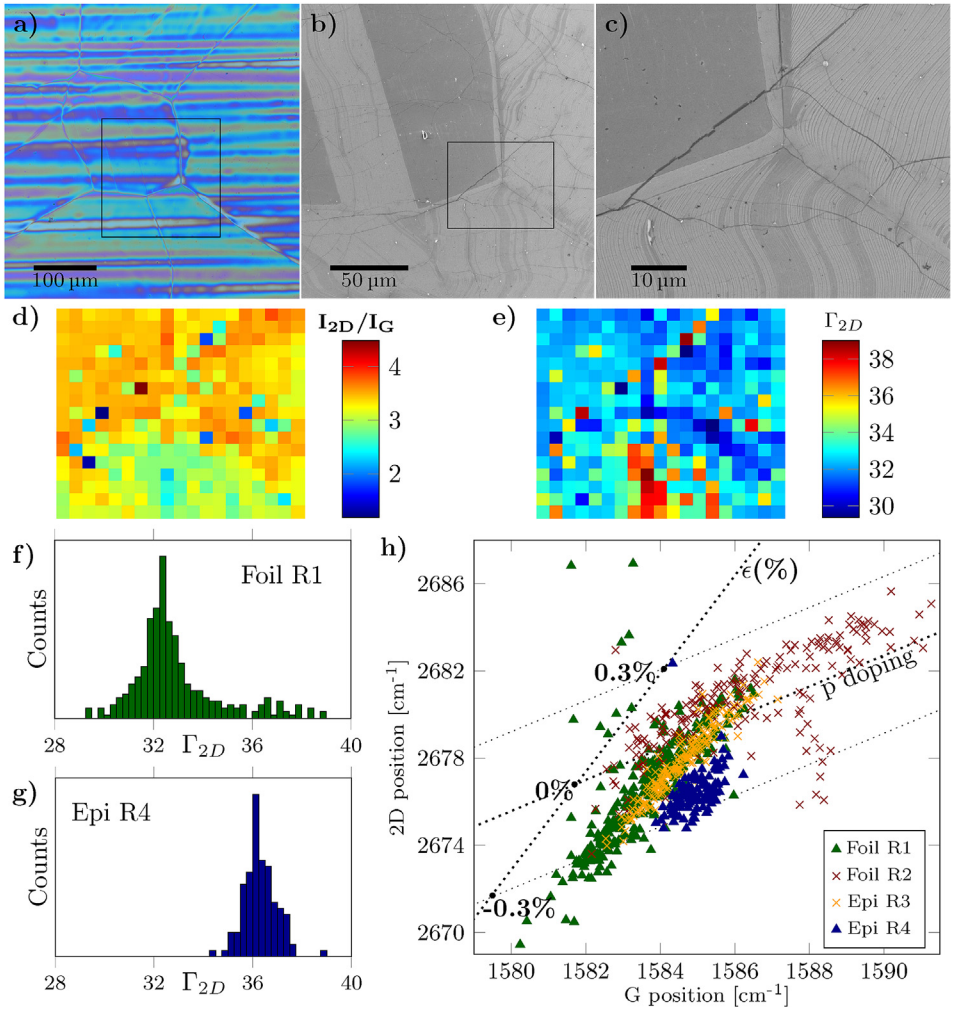

Fig. 4. a) Optical microscope image of the PMMA/Gr deposited onto a SiO_2/Si substrate using graphene grown on a Cu foil. **b)** In-lens SEM image of graphene on SiO_2/Si (after PMMA removal) taken in the area in the black rectangle in (a). **c)** Higher magnification SEM image corresponding to the area in the rectangle in (b). **d-e)** Raman maps (19 × 17 data points) of the 2D-to-G peak intensity ratio and 2D band FWHM (Γ_{2D}) acquired in the $54 \times 48\mu m$ region shown in (c). **f-g)** Histogram of the 2D band FWHM distribution for graphene grown on (f) Cu foils and (g) Cu film. **h)** 2D band position (ω_{2D}) versus G band position (ω_G) for various Raman maps acquired on graphene transferred on $SiO_2$from both Cu foils and epitaxial films. Reference axes for the mechanical strain (ε) and charge density have been obtained using models from Ref. [42]. R1, R2, R3, and R4 denote four different graphene regions used for Raman map acquisition. (A colour version of this figure can be viewed online.)

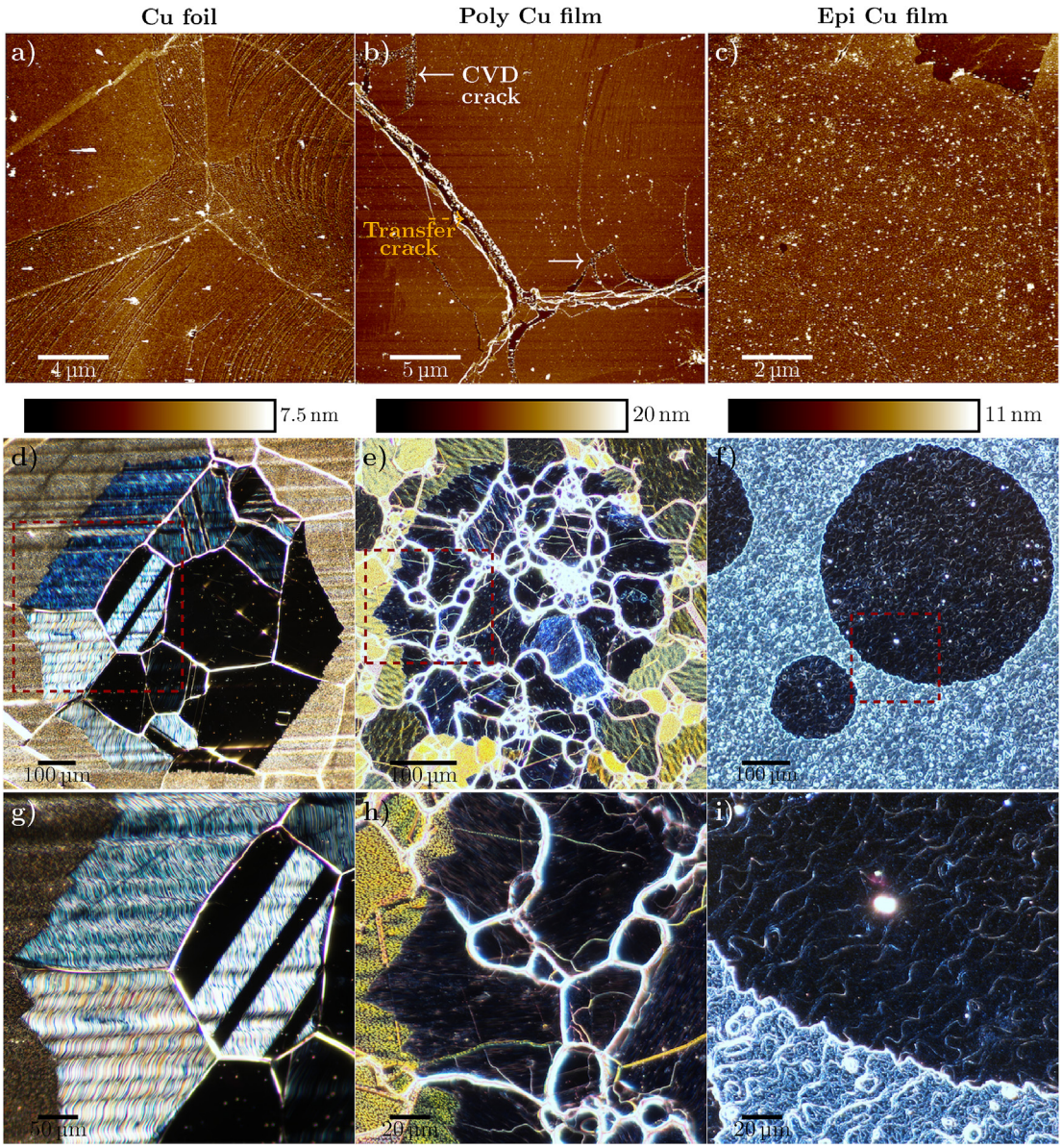

Fig. 5. Top panel: AFM images of graphene grown on Cu foil (left column), polycrystalline Cu film (center column), and epitaxial Cu film (right column) after being transferred onto a SiO_2/Si substrate. **Middle panel**: Dark field optical images of graphene as grown on Cu foil, polycrystalline Cu film, and epitaxial Cu film. **Bottom panel**: Higher magnification dark field optical images of the area in the dashed square in the middle panel. (A colour version of this figure can be viewed online.)

variations in graphene transferred from epitaxial Cu most likely arises from the superior planarity of graphene and the improved contact it forms with the underlying substrate, making it more sensitive to its surface roughness. Such observations are in good agreement with the work of *Couto* et al. which compared the effect of the target substrate on graphene's 2D band line width [46]. The spatial variation of strain at the Raman laser spot scale is probably a major factor explaining the fairly large range of 2D-to-G peak intensity ratio (observed in Fig. 4d) since averaging spectral components with slightly shifted 2D bands lead to a broader but less intense peak.

Fig. 4h displays the G band position ω_G with respect to the 2D band position ω_{2D}. Such plot enables to independently quantify the mechanical strain and the charge doping in graphene. Each green triangle data point (referred to as "Foil R1") in Fig. 4h corresponds to a pixel in the maps in Fig. 4d and e. This shows that most of the graphene region shown in Fig. 4c undergoes an in-plane strain varying from about −0.3% to +0.2% and a few localized regions possess a strain of about −0.4% or +0.6%.

A second map acquired in another region of the same sample (as referred to as "Foil R2") exhibits a distribution of data points presenting a narrower variation in ω_{2D} but a wider variation of ω_G. Such distribution is indicative of larger charge doping inhomogeneities which can stem from several origins: (i) graphene topside exposure to PMMA residues or oxygen and moisture adsorbed from the atmosphere [47,48], (ii) graphene coupling with the underlying SiO_2/Si substrate which has trapped charges and dangling bonds [42,49], and/or (iii) residual ions trapped at the Gr/SiO_2 interface during the Cu etching and PMMA/Gr rinsing process steps.

The doping from the graphene topside does not seem to be the major contribution responsible for the doping spatial variation since it should be rather constant for the different graphene regions within a given sample or different Raman single-point acquisitions within a given map. To better understand the origin of the doping

variations, two additional Raman maps (of similar dimensions) have been acquired on graphene grown on epitaxial Cu films and transferred onto SiO_2/Si. ω_G and ω_{2D} data, referred to as "Epi R3″ and "Epi R4", are displayed in Fig. 4h. Remarkably, these data exhibit a better clustering which indicates smaller variations in terms of strain and charge doping compared with graphene grown on Cu foils. Therefore, it is likely that the doping variations is caused by Cu foil larger features (e.g Cu grain boundary grooves) imprinted in the PMMA/Gr stack. These features tend to retain a certain amount of water from the last rinsing bath once graphene is transferred onto the final substrate. These trapped/stagnant water pockets formed at the Gr/SiO_2interface take a longer time to percolate/evaporate and can lead, to some extent, to a sedimentation process of the ionic species which results in graphene doping. It is also likely that the smaller Cu surface features (e.g. step edges) contribute to the doping variations as they impact the planarity of graphene on the final substrate, and hence, its proximity with dangling bonds and trapped charges present in the underlying substrate.

The planar aspect of graphene once transferred onto the target substrate can be assessed using atomic force microscopy (AFM). Fig. 5a–c have been acquired using a Bruker Icon with PeakForce Tapping mode with ScanAsyst at room temperature with a Peak Force set point of ~1 nN and a scan rate of ~1 Hz. Fig. 5a has been acquired in the region shown in Fig. 4c where graphene was grown at the mergence of three adjacent Cu grains. The AFM image clearly shows the graphene wrinkles and the remnants of the Cu step edges that were present on the Cu grains at the bottom and at the right of the image. The Cu surface step bunching taking place underneath graphene has been attributed to Cu atoms migration driven by relaxation mechanisms to mitigate graphene's compressive strain or local bending energy [50,51].

Fig. 5b also corresponds to the mergence of 3 individual Cu grains as shown in the area indicated by a white dashed rectangle in Fig. 2 (bottom panel). The extra surface area of graphene that grew in the Cu grain boundary groove and turned into a wrinkle can be clearly observed. AFM constitutes a useful tool to distinguish cracks that formed during the CVD process from cracks that formed during the transfer process. Cracks present in as-grown graphene are typically filled/covered with PMMA during the transfer process. When the PMMA/Gr stack is deposited on the final substrate, the PMMA present in the graphene cracks comes in direct contact with the $SiO_2$and leaves some residues after the PMMA removal. Such residues can easily be observed in Fig. 5b (white arrows). In contrast, cracks formed during the transfer process are usually cleaner as graphene used to be present between the PMMA and SiO_2before graphene gets washed away (as indicated by the orange arrow). The superior Cu surface morphology of epitaxial Cu films leads to almost no rippling in graphene once transferred as shown by the AFM image in Fig. 5c which has been acquired in the region marked by the dashed white rectangle in Fig. 3 (bottom panel, right column).

The formation of transfer-induced wrinkles in the transferred graphene film can be easily predicted by observing the larger Cu features (e.g. Cu grain boundary grooves or rolling striations) with a traditional optical microscope prior to the transfer process. Graphene nanometer-scale ripples, on the other hand, are the result of smaller Cu features (i.e. Cu step-edges) which usually require SEM or AFM to be properly observed. As shown in the top panel of Fig. 5, such rippling can drastically vary from one Cu grain to another. The dimensions of the Cu steps and terraces depend on various factors including the Cu surface curvature (especially near the Cu grain boundary grooves), the Cu surface crystalline orientation, and the number of graphene layers. Dark field (DF) optical microscopy is found to be a rapid and convenient route to anticipate the planar aspect of graphene prior to initiating the transfer process. Dark field imaging has previously been demonstrated to be useful to locate individual graphene domains on the Cu surface, distinguish single layer from multilayer regions, and observe local Cu oxidation which highlights graphene grain boundaries and other gas permeable defects [52,53]. Directly probing the graphene planar aspect on the catalytic substrate constitutes an asset when considering the fabrication of large arrays of devices with high performance as graphene rippling can drastically impair graphene's transport properties [54].

The middle and bottom panels of Fig. 5 show the DF optical images of graphene-coated Cu foils (left column), polycrystalline Cu film (middle column), and epitaxial Cu film (right column). Dark field imaging of Cu foils reveals various color shades and brightness levels caused by a disparity in Cu step bunching. Such contrast patchwork comes from the variety of Cu grain crystallographic orientations including Cu(100), Cu(101), and Cu(111) [32]. The more uniform color contrast in polycrystalline Cu films comes from the fact that most grains have the same Cu surface crystallographic orientation (i.e. Cu(111)) but exhibit a random in-plane orientation. The graphene-coated epitaxial Cu film appears darker because the surface has a low surface roughness, Cu(111) is a low index surface leading to minimal steps, and Cu terraces are horizontal, minimizing the amount of light reflected towards the microscope lens. Supporting Information S3 shows that the 3D optical profilometer can also serve as a rapid and non-destructive tool to predict the formation of ripples (and get an insight into their dimensions) prior to the transfer process.

3. Conclusion

In summary, we show that the Cu substrate morphology is a key process parameter to consider when developing a controllable, reliable and successful transfer process. Cu surface morphology endows graphene a non-planar aspect which is maintained by the mechanical support throughout the entire transfer process. The superior planarity of graphene grown on epitaxial Cu film yields a more conformal contact with the final substrate which results in improved adhesion and reduces graphene degradation during the transfer process. In contrast, polycrystalline Cu templates result in graphene exhibiting substantial out-of-plane deformations that are prone to cause cracking, wrinkling, non-uniform strain and doping variations. We also show that the graphene sub-micrometer ripples, which are caused by step bunching of the Cu surface, are one of the main factor responsible for strain and doping variations in transferred graphene. Although this study was primarily based on the widely used wet PMMA-based transfer method, our findings represent fundamental issues that apply to any transfer protocols, regardless of the material used as mechanical support, the Cu/graphene separation method, or the nature of the substrate. These results suggest the Cu template smoothness/flatness represent an important figure of merit for the graphene synthesis when aiming to develop controllable, reliable, reproducible, and large-scale fabrication of advanced technologies based on transferred graphene.

Declaration of competing interest

The authors declare that they have no known competing financial interests or personal relationships that could have appeared to influence the work reported in this paper.

CRediT authorship contribution statement

Benjamin Huet: Conceptualization, Methodology, Investigation, Visualization, Writing - review & editing. **Jean-Pierre Raskin:**

Resources. **David W. Snyder:** Resources, Writing - review & editing, Supervision. **Joan M. Redwing:** Resources, Writing - review & editing, Supervision, Funding acquisition.

Acknowledgements

The authors acknowledge the financial support of the National Science Foundation (NSF) through the Penn State 2D Crystal Consortium - Materials Innovation Platform (2DCC-MIP) under NSF cooperative agreement DMR-1539916. B.H. was also supported by the B.A.E.F. and by the WBI world excellence fellowships for one year at Penn State University. We gratefully acknowledge the Applied Research Laboratory (ARL), the Nanofabrication Laboratory and the Materials Characterization Lab (MCL) platforms of Penn State University for the CVD and characterization equipment.

Appendix A. Supplementary data

Supplementary data to this article can be found online at https://doi.org/10.1016/j.carbon.2020.02.074.

References

[1] Luca Banszerus, Michael Schmitz, Stephan Engels, Jan Dauber, Martin Oellers, Federica Haupt, Kenji Watanabe, Takashi Taniguchi, Bernd Beschoten, Christoph Stampfer, Ultrahigh-mobility graphene devices from chemical vapor deposition on reusable copper, Sci. Adv. 1 (2015).
[2] Young Duck Kim, Hakseong Kim, Yujin Cho, Ji Hoon Ryoo, Cheol-Hwan Park, Pilkwang Kim, Yong Seung Kim, Sunwoo Lee, Yilei Li, Seung-Nam Park, Yong Shim Yoo, Duhee Yoon, Vincent E. Dorgan, Eric Pop, Tony F. Heinz, James Hone, Seung-Hyun Chun, Hyeonsik Cheong, Sang Wook Lee, Myung-Ho Bae, Yun Daniel Park, Bright visible light emission from graphene, Nat. Nanotechnol. 10 (2015) 676.
[3] M. Hammad, J.-J. Adjizian, C.-H. Sacré, B. Huet, J.-C. Charlier, J.-P. Raskin, T. Pardoen, Adhesionless and near-ideal contact behavior of graphene on Cu thin film, Carbon 122 (Supplement C) (2017) 446–450.
[4] K.S. Novoselov, V.I. Falko, L. Colombo, P.R. Gellert, M.G. Schwab, K. Kim, A roadmap for graphene, Nature 490 (2012) 192.
[5] Amaia Zurutuza, Claudio Marinelli, Challenges and opportunities in graphene commercialization, Nat. Nanotechnol. 9 (2014) 730–734.
[6] Guoli Li, Nicolas André, Benjamin Huet, Thibault Delhaye, Nicolas Reckinger, Laurent A. Francis, Lei Liao, Jean-Pierre Raskin, Yun Zeng, Denis Flandre, Enhanced ultraviolet photoresponse in a graphene-gated ultra-thin si-based photodiode, J. Phys. D Appl. Phys. 52 (24) (apr 2019) 245101.
[7] Benjamin Huet, Jean-Pierre Raskin, Pressure-controlled chemical vapor deposition of single-layer graphene with millimeter-size domains on thin copper film, Chem. Mater. 29 (2017) 3431–3440.
[8] Benjamin Huet, Jean-Pierre Raskin, Role of Cu foil in-situ annealing in controlling the size and thickness of CVD graphene domains, Carbon 129 (2018) 270–280.
[9] Benjamin Huet, Xiaotian Zhang, Joan M. Redwing, David W. Snyder, Jean-Pierre Raskin, Multi-wafer batch synthesis of graphene on cu films by quasi-static flow chemical vapor deposition, 2D Mater. 6 (4) (2019), 045032.
[10] Mingguang Chen, Robert C. Haddon, Ruoxue Yan, Elena Bekyarova, Advances in transferring chemical vapour deposition graphene: a review, Mater. Horiz. 4 (2017) 1054–1063.
[11] Keun Soo Kim, Yue Zhao, Houk Jang, Sang Yoon Lee, Jong Min Kim, Kwang S. Kim, Jong-Hyun Ahn, Philip Kim, Jae-Young Choi, Byung Hee Hong, Large-scale pattern growth of graphene films for stretchable transparent electrodes, Nat. Lett. 457 (2009) 706–710.
[12] Ji Won Suk, Alexander Kitt, Carl W. Magnuson, Yufeng Hao, Samir Ahmed, Jinho An, Anna K. Swan, Bennett B. Goldberg, Rodney S. Ruoff, Transfer of CVD-grown monolayer graphene onto arbitrary substrates, ACS Nano 5 (2011) 6916–6924.
[13] Alfonso Reina, Hyungbin Son, Liying Jiao, Ben Fan, Mildred S. Dresselhaus, ZhongFan Liu, Jing Kong, Transferring and identification of single- and few-layer graphene on arbitrary substrates, J. Phys. Chem. C 112 (2008) 17741–17744.
[14] Matthew J. Allen, Vincent C. Tung, Lewis Gomez, Zheng Xu, Li-Min Chen, Kurt S. Nelson, Chongwu Zhou, Richard B. Kaner, Yang Yang, Soft transfer printing of chemically converted graphene, Adv. Mater. 21 (20) (2009) 2098–2102.
[15] Tuqeer Nasir, Bum Jun Kim, Kwan-Woo Kim, Sang Hoon Lee, Hyung Kyu Lim, Dong Kyu Lee, Byung Joo Jeong, Hak Chul Kim, Hak Ki Yu, Jae-Young Choi, Design of softened polystyrene for crack- and contamination-free large-area graphene transfer, Nanoscale 10 (2018) 21865–21870.
[16] Liubov A. Belyaeva, Wangyang Fu, Hadi Arjmandi-Tash, Grégory F. Schneider, Molecular caging of graphene with cyclohexane: transfer and electrical transport, ACS Cent. Sci. 2 (12) (2016) 904–909.
[17] Jin-Yong Hong, Yong Cheol Shin, Ahmad Zubair, Yunwei Mao, Tomás Palacios, Mildred S. Dresselhaus, Sung Hyun Kim, Jing Kong, A rational strategy for graphene transfer on substrates with rough features, Adv. Mater. 28 (12) (2016) 2382–2392.
[18] Wei Sun Leong, Haozhe Wang, Jingjie Yeo, J. Francisco, Martin-Martinez, Ahmad Zubair, Pin-Chun Shen, Yunwei Mao, Tomas Palacios, Markus J. Buehler, Jin-Yong Hong, Jing Kong, Paraffin-enabled graphene transfer, Nat. Commun. 10 (2019) 867.
[19] Di-Yan Wang, I-Sheng Huang, Po-Hsun Ho, Shao-Sian Li, Yun-Chieh Yeh, Duan-Wei Wang, Wei-Liang Chen, Yu-Yang Lee, Yu-Ming Chang, Chia-Chun Chen, Chi-Te Liang, Chun-Wei Chen, Clean-lifting transfer of large-area residual-free graphene films, Adv. Mater. 25 (32) (2013) 4521–4526.
[20] Yu Wang, Yi Zheng, Xiangfan Xu, Emilie Dubuisson, Qiaoliang Bao, Jiong Lu, Kian Ping Loh, Electrochemical delamination of cvd-grown graphene film: toward the recyclable use of copper catalyst, ACS Nano 5 (12) (2011) 9927–9933.
[21] Jae-Young Choi, A stamp for all substrates, Nat. Nanotechnol. 8 (2013) 311.
[22] Jie Song, Fong-Yu Kam, Png Rui-Qi, Wei-Ling Seah, Jing-Mei Zhuo, Geok-Kieng Lim, Peter K.H. Ho, Lay-Lay Chua, A general method for transferring graphene onto soft surfaces, Nat. Nanotechnol. 8 (2013) 356.
[23] Andres Castellanos-Gomez, Michele Buscema, Rianda Molenaar, Vibhor Singh, Laurens Janssen, Herre S.J. van der Zant, Gary A. Steele, Deterministic transfer of two-dimensional materials by all-dry viscoelastic stamping, 2D Mater. 1 (1) (2014), 011002.
[24] Nan Liu, Zhonghuai Pan, Lei Fu, Chaohua Zhang, Boya Dai, Zhongfan Liu, The origin of wrinkles on transferred graphene, Nano Res 4 (2011) 996–1004.
[25] Xuesong Li, Yanwu Zhu, Weiwei Cai, Mark Borysiak, Boyang Han, David Chen, Richard D. Piner, Luigi Colombo, Rodney S. Ruoff, Transfer of large-area graphene films for high-performance transparent conductive electrodes, Nano Lett. 9 (2009) 4359–4363.
[26] Azadeh Jafari, Mahmood Ghoranneviss, Mojtaba Gholami, N. Mostahsan, The role of deposition temperature and catalyst thickness in graphene domains on cu, Int. Nano Lett. 5 (4) (2015) 199–204.
[27] A. Ismach, C. Druzgalski, S. Penwell, A. Schwartzberg, M. Zheng, A. Javey, J. Bokor, Y. Zhang, Direct chemical vapor deposition of graphene on dielectric surfaces, Nano Lett. 10 (2010) 1542–1548.
[28] C.-Y. Su, A.-Y. Lu, C.-Y. Wu, Y.-T. Li, K.-K. Liu, W. Zhang, S.-Y. Lin, Z.-Y. Juang, Y.-L. Zhong, F.-R. Chen, L.-J. Li, Direct formation of wafer scale graphene thin layers on insulating substrates by chemical vapor deposition, Nano Lett. 11 (2011) 3612–3616.
[29] C.A. Howsare, X. Weng, V. Bojan, D. Snyder, J.A. Robinson, Substrate considerations for graphene synthesis on thin copper films, Nanotechnology 23 (2012).
[30] J.L. Qi, K. Nagashio, T. Nishimura, A. Toriumi, The crystal orientation relation and macroscopic surface roughness in hetero-epitaxial graphene grown on cu/mica, Nanotechnology 25 (18) (2014) 185602.
[31] R.M. Jacobberger, M.S. Arnold, Graphene growth dynamics on epitaxial copper thin films, Chem. Mater. 25 (2013) 871–877.
[32] Benjamin Huet, Jean-Pierre Raskin, Role of the cu substrate in the growth of ultra-flat crack-free highly-crystalline single-layer graphene, Nanoscale 10 (2018) 21898–21909.
[33] Baoshan Hu, Hiroki Ago, Yoshito Ito, Kenji Kawahara, Masaharu Tsuji, Eisuke Magome, Kazushi Sumitani, Noriaki Mizuta, Ken ichi Ikeda, Seigi Mizuno, Epitaxial growth of large-area single-layer graphene over cu(111)/sapphire by atmospheric pressure cvd, Carbon 50 (1) (2012) 57–65.
[34] Hiroki Ago, Kenji Kawahara, Yui Ogawa, Shota Tanoue, Mark A. Bissett, Masaharu Tsuji, Hidetsugu Sakaguchi, Roland J. Koch, Felix Fromm, Thomas Seyller, Katsuyoshi Komatsu, Kazuhito Tsukagoshi, Epitaxial growth and electronic properties of large hexagonal graphene domains on Cu(111) thin film, Appl. Phys. Express 6 (2013), 075101.
[35] David L. Miller, Mark W. Keller, Justin M. Shaw, Katherine P. Rice, Robert R. Keller, Kyle M. Diederichsen, Giant secondary grain growth in Cu films on sapphire, AIP Adv. 3 (2013), 082105.
[36] C. Jia, J. Jiang, L. Gan, X. Guo, Direct optical characterization of graphene growth and domains on growth substrates, Sci. Rep. 2 (1–6) (2012).
[37] Steven P. Koenig, Narasimha G. Boddeti, Martin L. Dunn, J. Scott Bunch, Ultrastrong adhesion of graphene membranes, Nat. Nanotechnol. 6 (9) (2011) 543–546.
[38] Rui He, Liuyan Zhao, Nicholas Petrone, Keun Soo Kim, Michael Roth, James Hone, Philip Kim, Abhay Pasupathy, Aron Pinczuk, Large physisorption strain in chemical vapor deposition of graphene on copper substrates, Nano Lett. 12 (5) (2012) 2408–2413.
[39] Merijntje S. Bronsgeest, Nedjma Bendiab, Shashank Mathur, Amina Kimouche, Harley T. Johnson, Johann Coraux, Pascal Pochet, Strain relaxation in cvd graphene: wrinkling with shear lag, Nano Lett. 15 (8) (2015) 5098–5104.
[40] Gerald V. Troppenz, Marc A. Gluba, Marco Kraft, Jorg Rappich, Norbert H. Nickel, Strain relaxation in graphene grown by chemical vapor deposition, J. Appl. Phys. 114 (21) (2013) 214312.
[41] L.F. Francis, A.V. Mccormick, D.M. Vaessen, J.A. Payne, Development and measurement of stress in polymer coatings, J. Mater. Sci. 37 (22) (2002) 4717–4731.
[42] Ji Eun Lee, Gwanghyun Ahn, Jihye Shim, Young Sik Lee, Sunmin Ryu, Optical separation of mechanical strain from charge doping in graphene, Nat. Com. 3 (2012).
[43] Andrea C. Ferrari, Denis M. Basko, Raman spectroscopy as a versatile tool for

studying the properties of graphene, Nat. Nanotechnol. 8 (2013) 235–246.
[44] C. Neumann, S. Reichardt, P. Venezuela, M. Drogeler, L. Banszerus, M. Schmitz, K. Watanabe, T. Taniguchi, F. Mauri, B. Beschoten, S.V. Rotkin, C. Stampfer, Raman spectroscopy as probe of nanometre-scale strain variations in graphene, Nat. Commun. 6 (2015) 8429.
[45] Qing Hua Wang, Zhong Jin, Ki Kang Kim, Andrew J. Hilmer, L. Geraldine, C. Paulus, Chih-Jen Shih, Moon-Ho Ham, Javier D. Sanchez-Yamagishi, Kenji Watanabe, Takashi Taniguchi, Jing Kong, Pablo Jarillo-Herrero, Michael S. Strano, Understanding and controlling the substrate effect on graphene electron-transfer chemistry via reactivity imprint lithography, Nat. Chem. 4 (2012) 724.
[46] Nuno J.G. Couto, Davide Costanzo, Stephan Engels, Dong-Keun Ki, Kenji Watanabe, Takashi Taniguchi, Christoph Stampfer, Francisco Guinea, Alberto F. Morpurgo, Random strain fluctuations as dominant disorder source for high-quality on-substrate graphene devices, Phys. Rev. X 4 (2014), 041019.
[47] Ruiheng Li, Zongyi Li, Elias Pambou, Philipp Gutfreund, Thomas A. Waigh, John R.P. Webster, Jian R. Lu, Determination of pmma residues on a chemical-vapor-deposited monolayer of graphene by neutron reflection and atomic force microscopy, Langmuir 34 (5) (2018) 1827–1833.
[48] Sunmin Ryu, Li Liu, Stephane Berciaud, Young-Jun Yu, Haitao Liu, Philip Kim, George W. Flynn, Louis E. Brus, Atmospheric oxygen binding and hole doping in deformed graphene on a SiO2 substrate, Nano Lett. 10 (12) (2010) 4944–4951.
[49] S.D. Costa, J. Ek Weis, O. Frank, M. Fridrichova, M. Kalbac, Monitoring the doping of graphene on SiO2/si substrates during the thermal annealing process, RSC Adv. 6 (2016) 72859–72864.
[50] Jin Hyoun Kang, Joonhee Moon, Dong Jin Kim, Yooseok Kim, Insu Jo, Cheolho Jeon, Jouhahn Lee, Byung Hee Hong, Strain relaxation of graphene layers by cu surface roughening, Nano Lett. 16 (10) (2016) 5993–5998.
[51] Ding Yi, Da Luo, Zhu-Jun Wang, Jichen Dong, Xu Zhang, Marc-Georg Willinger, Rodney S. Ruoff, Feng Ding, What drives metal-surface step bunching in graphene chemical vapor deposition? Phys. Rev. Lett. 120 (2018) 246101.
[52] X.H. Kong, H.X. Ji, R.D. Piner, H.F. Li, C.W. Magnuson, C. Tan, A. Ismach, H. Chou, R.S. Ruoff, Non-destructive and rapid evaluation of chemical vapor deposition graphene by dark field optical microscopy, Appl. Phys. Lett. 103 (4) (2013), 043119.
[53] Dong Ding, Hiroki Hibino, Hiroki Ago, Grain boundaries and gas barrier property of graphene revealed by dark-field optical microscopy, J. Phys. Chem. C 122 (1) (2018) 902–910.
[54] Shikai Deng, Vikas Berry, Wrinkled, rippled and crumpled graphene: an overview of formation mechanism, electronic properties, and applications, Mater. Today 19 (4) (2016) 197–212.